Supplementary

Chemically engineered alloy anode enabling fully reversible conversion reaction: Design of C-Sn bonded aerofilm anode

Sun-Sik Kim,[‡a] *Chenrayan Senthil,*[‡a] *Sung Mi Jung*[b] *and Hyun Young Jung*[*ac]

[a] Department of Energy Engineering, Gyeongsang National University, Jinju-si, Gyeongnam 52725, South Korea

[b] Environmental Fate & Exposure Research Group, Korea Institute of Toxicology, Jinju-si, Gyeongnam 52834, South Korea

[c] Future Convergence Technology Research Institute, Gyeongsang National University, Jinju-si, Gyeongnam 52725, South Korea

* To whom correspondence should be addressed. E-mail: hyjung@gnu.ac.kr (Prof. H.Y. Jung)

‡ Authors equally contributed

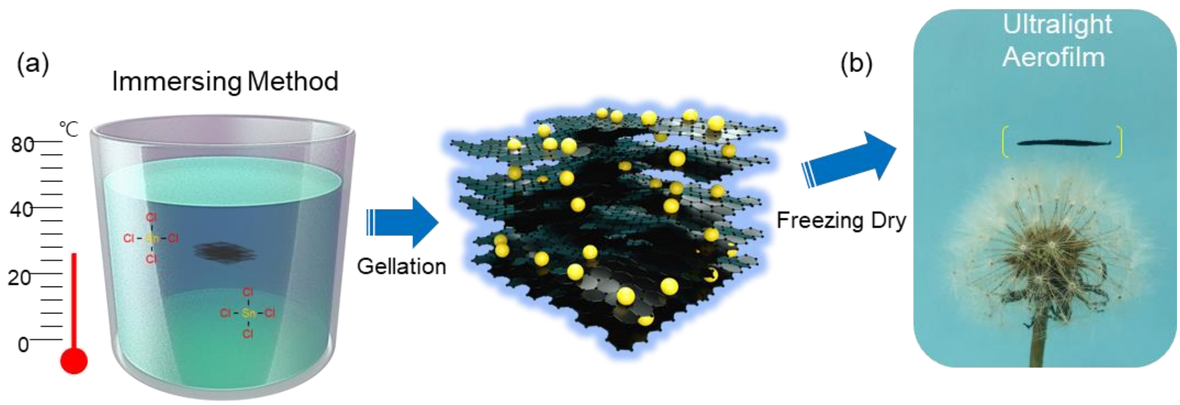

Fig. S1. (a) Formation of C-Sn bonded aerofilm anode by a simple immersion technique. (b) Ultralight nature of aerofilm anode placed over a dandelion flower.

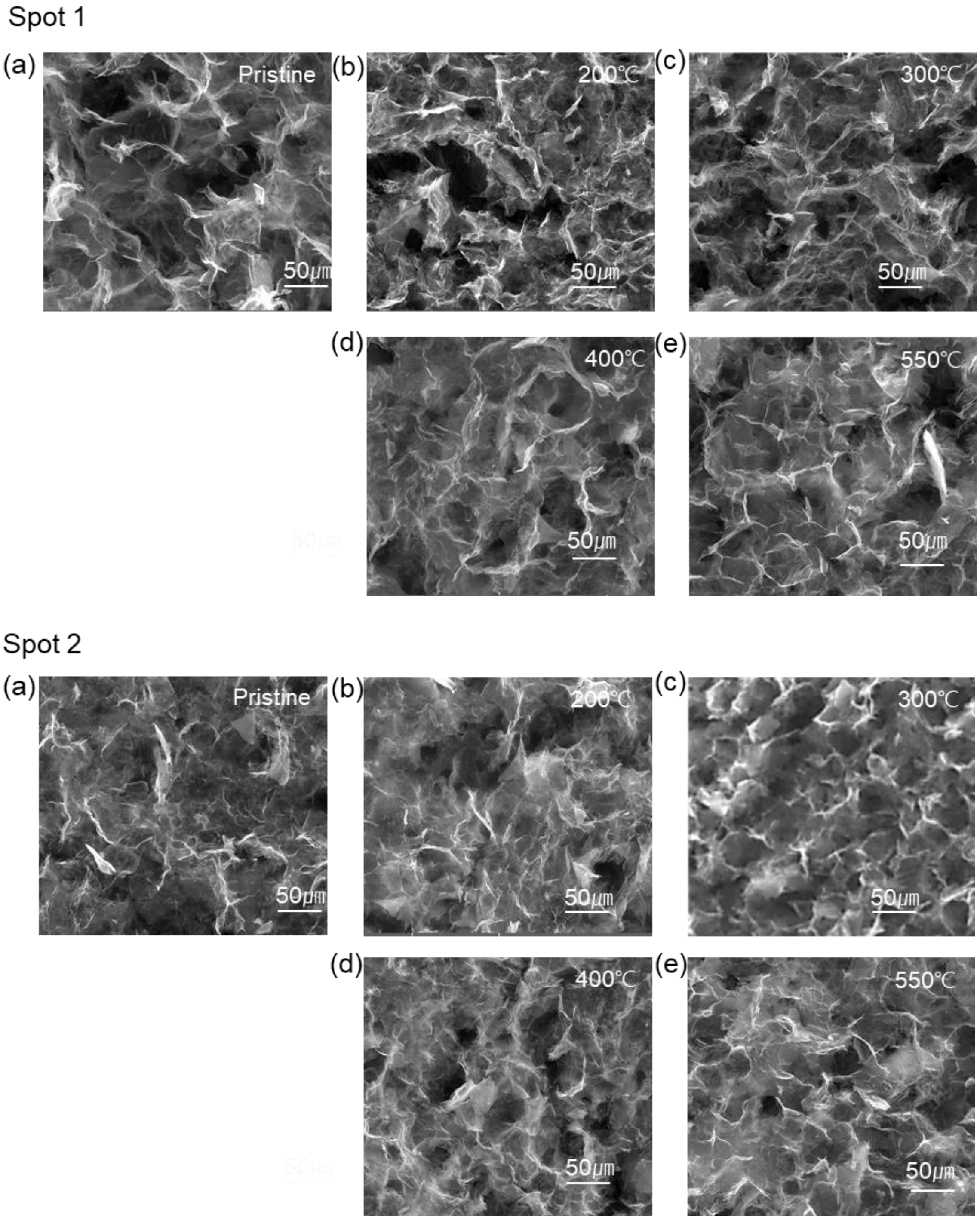

Fig. S2. SEM micrographs at different spots (spot 1 and spot 2) depicting the morphological understanding in SnO_2 aerofilm anode annealed at 200, 300, 400, and 550°C compared with no annealed anode.

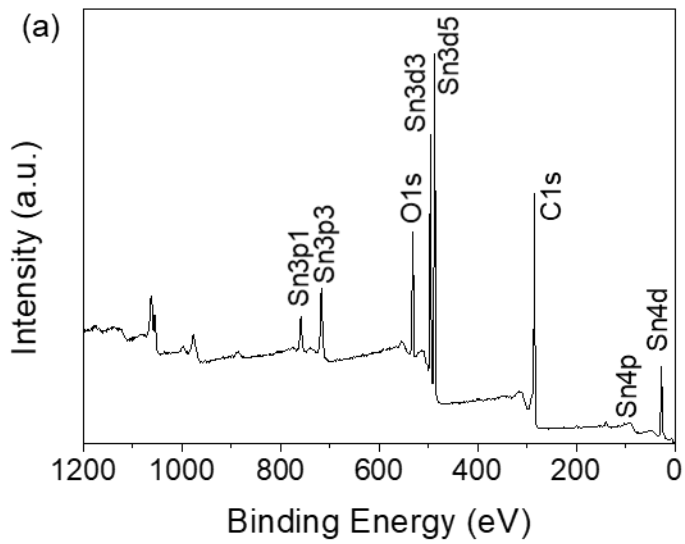

Fig. S3. (a) XPS survey for C-Sn bonded aerofilm anode.

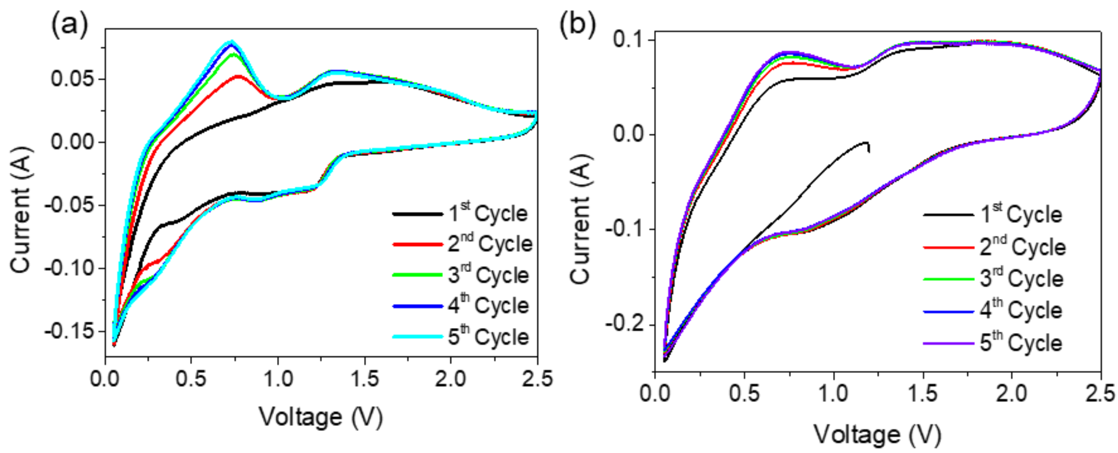

Fig. S4. Cyclic voltammetry curves during the initial five cycles at 1mV s^{-1} (a) C-O-Sn and (b) C-Sn bonded anode.

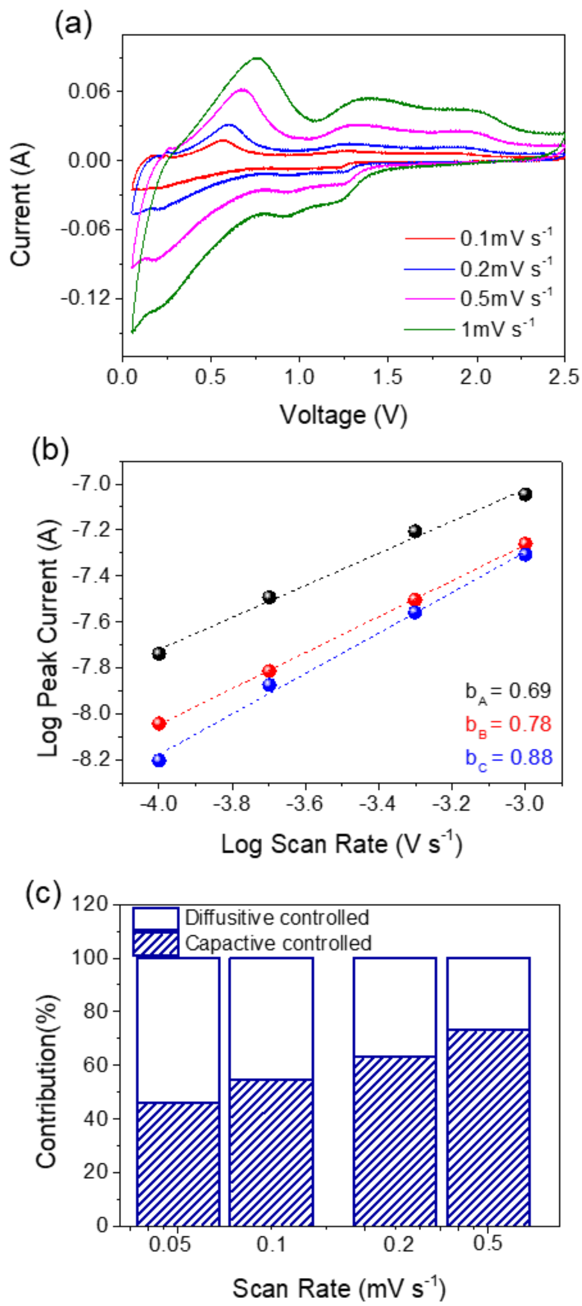

Fig. S5. (a) Cyclic voltammetry curves of C-O-Sn bonded anode at various scan rates of 0.1, 0.2, 0.5, 1.0 mV^{-1}. (b) b-value from (a). (c) Diffusion and capacitive controlled Li storage contribution.

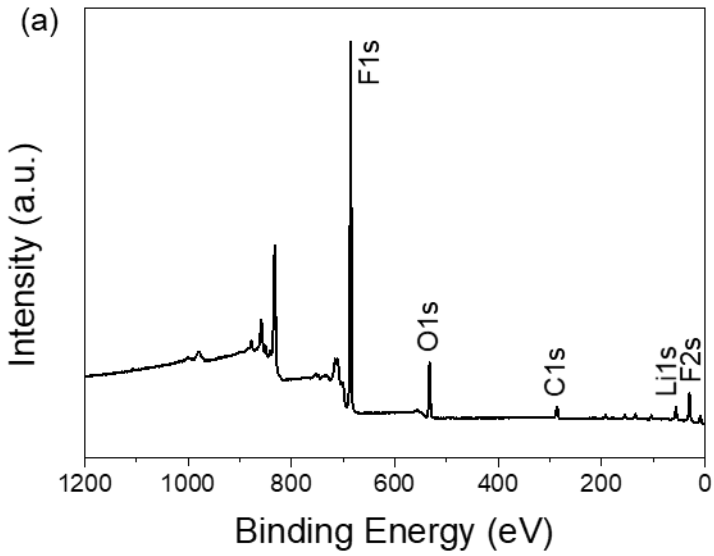

Fig. S6. XPS survey of cycled and lithiated C-Sn bonded aerofilm anode.

Cell parameters

The specific capacity was calculated based on the mass of SnO_2, which is considered as the active material. The details of cell parameters are as follows,

Mass of G-SnO_2 : 1.56 – 2.1 mg/cm^2,

Mass of SnO_2 : 1.11 g – 1.49 mg/cm^2,

Current rate : 1 C (0.79 A/g based on theoretical capacity of SnO_2).

Table S1. Comparison of resistance and diffusion coefficient for C-Sn and C-O-Sn aerofilm anode on EIS.

	Rs (kΩ)	Rsei (kΩ)	Rct (kΩ)	D_{Li} (cm^2 s^{-1})
C-O-Sn	12.1	0.75	0.36	1.67E-11
C-Sn	6.73	0.49	0.153	1.54E-10

Table S2. Electrochemical performance comparison of previously reported graphene-SnO_2 composite electrode for Li-ion battery.

Electrode (Content)	**Synthetic method**	**Voltage Window (V)**	**1st Cycle Capacity (mAh g^{-1})**	**2nd Cycle Capacity (mAh g^{-1})**	**Condition (A g^{-1})**	**Retention rate (1st and 2nd Cycle)**	**Ref.**
Graphene-SnO_2 aerofilm	**Immersing**	**0.005~2.5**	**1183**	**1158**	**0.158**	**98%**	**Our Work**
			958	**951**	**0.790**	**99%**	
Graphene/Sn @ carbonaceous foam	Hydrothermal	0.001~3	~1300	~800	0.1	62%	S1
Sn@3D graphene networks	Freeze drying and CVD	0.005~3	~1800	~1200	0.2	67%	S2
SnO_2 quantum dots@GO	Hydrothermal	0.01~3	~1500	~1000	0.1	67%	S3
F-doped SnO_2@rGO	Hydrothermal	0.01~3	~2000	~1250	0.1	63%	S4
SnO_2/graphene	hydrolysis	0.01~2	~980	~920	0.067	94%	S5
SnO_2/CNT-GN composite	Hydrothermal	0.01~3	~1800	~1100	0.2	61%	S6
3D annealed SnO_2/ graphene foams	Hydrothermal	0.01~3	~1650	~1000	0.2	61%	S7
Tin graphene tube	Hydrothermal	0.01~2.5	~1300	~900	0.2	69%	S8
N-Doped Gr_SnO_2	Solution	0.05~3	~1450	~900	0.05	62%	S9
Graphene Nanoribbon and Nanostructured SnO_2	Solution refluxing	0.01~2.5	~1500	~1110	0.1	74%	S10
SnO_2/RGO	Hydrothermal	0.01~3	~1542	~837	0.5	54%	S11

Table S3. Cycle stability comparison of previously reported graphene-SnO_2 composite electrode for Li-ion battery.

Electrode (Content)	Voltage Window (V)	Cyclability (mAh g^{-1})	Rate performance (mAh g^{-1})	Ref.
Graphene-SnO_2 aerofilm	**0.005~2.5**	**1255 (200cycle at 158mA g^{-1})**	**553 (1500cycle at 0.79A g^{-1})**	**Our Work**
Graphene/Sn@carbonaceous foam	0.001~3	777 (100 cycles at 100 mA g^{-1})	506 (500cycle at 400 mA g^{-1}) 270 (500cycle at 3200 mA g^{-1})	S1
Graphene/Sn @ carbonaceous foam	0.005~3	1,089 (100cycle at 200mA g^{-1})	459 (at 5 A/g) 270 (at 10 A g^{-1})	S2
Sn@3D graphene networks	0.01~3	112 (100 cycles at 100 mA g^{-1})	417 (2,000 cycle at 2 A g^{-1})	S3
SnO_2 quantum dots@GO	0.01~3	1,037 (150 cycles at 100 mA g^{-1})	860 (at 1 A/g) 770 (at 2 A g^{-1})	S4
F-doped SnO_2@rGO	0.01~2	840 (30 cycle at 67mA g^{-1})	590 (50cycle at 400mA g^{-1}) 270 (50cycle at 1000mA g^{-1})	S5
SnO_2/graphene	0.01~3	809 (100cycle at 200mA g^{-1})	787 (at 500mA g^{-1})	S6
SnO_2/CNT-GN composite	0.01~3	984.2 (at 200mA g^{-1})	533.7 (150cycle at 1A g^{-1})	S7
3D annealed SnO_2/graphene sheet foams	0.01~2.5	916 (500cycle at 200mA g^{-1})	810 (500cycle at 0.5A g^{-1})	S8
tin graphene tube	0.05~3	894 (at 50mA g^{-1})	-	S9
N-Doped Gr_SnO_2	0.01~2.5	825 (50cycle at 100mA g^{-1})	580 (at 2A g^{-1})	S10
Graphene Nanoribbon and Nanostructured SnO_2	0.01~3	708 (150cycle at 500mA g^{-1})	520 (at 1A g^{-1})	S11

Table S4. Comparison of SnO_2 aerofilm anode with commercial graphite

Electrode (Content)	Voltage Window (V)	Cyclability (mAh g^{-1})	Rate performance (mAh g^{-1})	Ref.
Commercial graphite	0~2	260 (100cycle at 200mA g^{-1})	153 (300cycle at 1A g^{-1})	S12
Graphene	0.01-3.5	540 (at 50mA g^{-1})	-	S13
CNT	0.01~3	460 (at 20mA g^{-1})	-	S14
N doping carbon	0.01~3	2053 (80cycle at 100mA g^{-1})	879 (1000cycle at 5A g^{-1})	S15
C-Sn bonded aerofilm	**0.005~2.5**	**1255 (200cycle at 158mA g^{-1})**	**553 (1500cycle at 0.79A g^{-1})**	**Our Work**

References

S1. B. Luo, T. Qiu, D. Ye, L. Wang, L. Zhi, Tin nanoparticles encapsulated in graphene backboned carbonaceous foams as high-performance anodes for lithium-ion and sodium-ion storage, Nano Energy 22 (2016) 232-240, https://doi.org/10.1016/j.nanoen.2016.02.024.

S2. J. Qin, C. He, N. Zhao, Z. Wang, C. Shi, E.-Z. Liu, J. Li, Graphene networks anchored with Sn@ graphene as lithium ion battery anode, ACS Nano 8 (2014) 1728-1738, https://doi.org/10.1021/nn406105n.

S3. K. Zhao, L. Zhang, R. Xia, Y. Dong, W. Xu, C. Niu, L. He, M. Yan, L. Qu, L. Mai, SnO2 Quantum dots@graphene oxide as a high-rate and long-life anode material for lithium-ion batteries, small 12 (2016) 588-594, https://doi.org/10.1002/smll.201502183.

S4. D. Cui, Z. Zheng, X. Peng, T. Li, T. Sun, L. Yuan, Fluorine-doped SnO2 nanoparticles anchored on reduced graphene oxide as a high-performance lithium ion battery anode, J. Power Sources 362 (2017) 20-26, https://doi.org/10.1016/j.jpowsour.2017.07.024.

S5. X. Wang, X. Zhou, K. Yao, J. Zhang, Z. Liu, A SnO2/graphene composite as a high stability electrode for lithium ion batteries, Carbon 49 (2011) 133-139, https://doi.org/10.1016/j.carbon.2010.08.052.

S6. M.-S. Wang, Z.-Q. Wang, Z.-L. Yang, Y. Huang, J. Zheng, X. Li, Carbon nanotube-graphene nanosheet conductive framework supported SnO2 aerogel as a high performance anode for lithium ion battery, Electrochim. Acta 240 (2017) 7-15, https://doi.org/10.1016/j.electacta.2017.04.031.

S7. M. Zhang, Z. Sun, T. Zhang, D. Sui, Y. Ma, Y. Chen, Excellent cycling stability with high SnO2 loading on a three-dimensional graphene network for lithium ion batteries, Carbon 102 (2016) 32-38, https://doi.org/10.1016/j.carbon.2016.02.032.

S8. A. Dhanabalan, X. Li, R. Agrawal, C. Chen, C. Wang, Fabrication and characterization of SnO2/graphene composites as high capacity anodes for Li-ion batteries, Nanomaterials 3 (2013) 606-614, https://doi.org/10.3390/nano3040606.

S9. R. Tian, Y. Zhang, Z. Chen, H. Duan, B. Xu, Y. Guo, H. Kang, H. Li, H. Liu, The effect of annealing on a 3D SnO 2/graphene foam as an advanced lithium-ion battery anode, Sci. Rep. 6 (2016) 1-9, https://doi.org/10.1038/srep19195 (2016).

S10. Z.-F. Li, Q. Liu, Y. Liu, F. Yang, L. Xin, Y. Zhou, H. Zhang, L. Stanciu, J. Xie, Facile preparation of graphene/SnO2 xerogel hybrids as the anode material in Li-ion batteries, ACS Appl. Mater. Interfaces 7 (2015) 27087-27095, https://doi.org/10.1021/acsami.5b05819.

S11. Q. Tan, Z. Kong, X. Chen, L. Zhang, X. Hu, M. Mu, H. Sun, X. Shao, X. Guan, M. Gao, Synthesis of SnO2/graphene composite anode materials for lithium-ion batteries, App. Surf. Sci. 485 (2019) 314-322. https://doi.org/10.1016/j.apsusc.2019.04.225.

S12. J.Kim, S.M.N.Jeghan, G.Lee, Superior fast-charging capability of graphite anode via facile surface treatment for lithium-ion batteries, Microporous Mesoporous Mater. 305 (2020) 110325. https://doi.org/10.1016/j.micromeso.2020.110325.

S13. P.Lian, X.Zhu, S.Liang, Z.Li, W.Yang, H.Wang, Large reversible capacity of high quality graphene sheets as an anode material for lithium-ion batteries, Electrochim. Acta 55 (2010) 3909-3914. https://doi:10.1016/j.electacta.2010.02.025.

S14. A.S.Claye, J.E.Fischer, C.B.Huffman, A.G.Rinzler, R.E.Smalley, Solid-State Electrochemistry of the Li Single Wall Carbon Nanotube System, J. Electrochem. Soc. 147 (2000) 2845-2852.

S15. Y.Yang, S.Jin, Z.Zhang, Z.Du, H.Liu, J.Yang, H.Xu, H.Ji, Nitrogen-Doped Hollow Carbon Nanospheres for High-Performance Li-Ion Batteries, ACS Appl. Mater. Interfaces 9 (2017) 14180-14186. https://doi.org/10.1021/acsami.6b14840.